



Original Research / Orijinal Araştırma

Failure characteristics of surrounding rocks in coal seam mining roadway

Kömür madenlerindeki yeraltı yollarında yan kayaçların yenilme özellikleri

Xiaolei Wang^{a,*}^a Department of Mining Engineering, Luliang University, Lvliang 033001, China

Geliş-Received: 30 Nisan - April 2021 * Accepted: 26 Aralık - December 2021

A B S T R A C T

In order to provide technical support for grouting engineering of broken surrounding rock in roadway. Taking a certain mine in Jin coal mine area as a test mine, drilling TV and segmented water injection tests were used to detect the damage characteristics of surrounding rocks, and the numerical simulation of stress characteristics during the failure process was carried out. The research results show that the crack width of the surrounding rock can be reduced to four areas from the inside to the outside, and the crack widths are different. After the excavation of the roadway, the stress concentration occurs inside the coal and rock mass. With the excavation, the stress exceeds the strength of the coal and rock mass, and the failure occurs, and the stress concentration phenomenon continues to develop deep; the radial direction of the roadway is divided into four areas: completely broken zone, fracture reduction zone, fractured compression zone and proto-rock-like area.

Keywords: Mining engineering, Fissure, Surrounding rock of roadway, Numerical simulation

Introduction

During the mining of underground coal seams, the original stress was destroyed, and the stress formed a dynamic change process (Huang et al., 2021; Kang, 2021). During this change of stress, the surrounding rock of the roadway will inevitably be destroyed (Zhu et al., 2019). This change in the permeability characteristics of the surrounding rock occurs because the dynamic pressure of coal mining projects must have different stress characteristics in different parts of the surrounding rock of the roadway, and their varying damage characteristics will inevitably lead to different seepage characteristics in different parts of the roadway (Jia and Hu, 2020; Li et al., 2020a; Yu et al., 2021), which will be reflected by changes in the spatial permeability of the surrounding rock of the roadway (Zhu and Teng, 2021; Zhao and Fu, 2020). The seepage field in the rock is not only a channel for fissure water and gas, but also a channel for slurry flow during the control of surrounding rocks (Cheng et al., 2020; Chen, 2020; Ma et al., 2020). The partition failure characteristics of the surrounding rock in the roadway are of great significance to the quality of the grouting effect (Zhang et al., 2020a; Yang et al., 2020; Xu et al., 2019).

The theoretical analysis of failure and deformation of roadway broken body is mainly based on elastic-plastic theory (Xu and Gao, 2020). It is the basic theory to study the failure of roadway coal and rock mass. In the late 1930's, based on the Mohr Coulomb criterion, the chamber was simplified into an axisymmet-

ric isotropic and isobaric plane model, the relationship between stress, strain and support characteristics under elasticity and the mechanical strength of surrounding rock were analyzed, and the Kastner formula of plastic zone radius and stress was deduced. The surrounding rock plastic strain softening is introduced into the tunnel elastic-plastic solution based on stress release (Li et al., 2021; Li and Wang, 2020; Chen et al., 2020; Cai, 2020). At the same time, considering the softening characteristics and the surrounding rock expansion characteristics of residual strength, the elastic-plastic solution of circular tunnel is proposed. Many scholars consider the influence of residual strength of deep surrounding rock after failure, and put forward new opinions based on this (Wang, 2018; Zhang et al., 2020a; Wang et al., 2020a). On the basis of rock deformation weakening and residual deformation stage, the surrounding rock is regarded as a linear ideal residual model. The stress field in the plastic zone of surrounding rock is explained by using plastic mechanics and considering the damage zone, residual strength and support characteristics of roadway. Considering the characteristics of rock mass strength after roadway excavation, a theoretical calculation model is established. Considering the influence of strength softening and original rock stress (Cai, 2020; Li and Du., 2020; Cai et al., 2020; Chai et al., 2020), the surrounding rock structure is divided into deep and shallow support layers (Wang, 2019). The nonlinear brittle model is introduced and the surrounding rock is divided into three zones by using the unified strength theory (Chen et al., 2021). Based

* Corresponding author / Sorumlu yazar: llxywxi@126.com • <https://orcid.org/0000-0002-7273-2230>

on the influence of intermediate stress on surrounding rock, the plastic radius and analytical solution are deduced by using relevant rules. Based on the Mohr Coulomb criterion, the influence of expansion characteristics is considered (Wang et al., 2020b; Ren, 2020; Liu et al., 2020; Zuo et al., 2019).

In the mining process of working face, coal and rock mass are damaged due to the existence of support pressure and the influence of mining. Although the fracture development of coal and rock mass is analyzed, the specific distribution characteristics are not studied. In this paper, taking a mine in Shanxi Figure 1 as an experimental mine, the failure characteristics of surrounding rock are studied by numerical simulation, borehole television peeping and segmented water injection test.



Figure 1. Coal mine location

1. Materials and Methods

A mine in the Jin coal mine area is located in the northwest of Jincheng City. The mine’s production capacity is 1.8 Mt/a. The main mining coal seams are 3, 9, and 15. The thickness of the coal seams is 6 m, 1.5 m, and 2.4 m. The on-site monitoring is selected at the 4309 working face. No. 9 coal seam is mined in the working face, which is a near-horizontal coal seam. The coal seam is located in the Upper Carboniferous Taiyuan Formation. The roof of the working face is siltstone with a thickness of about 3.93 m. The thickness of the rock layer is 5.09 m, with corrugated bedding. The bottom of the coal seam is limestone with a thickness of about 0.45 m, which is a direct bottom, and the basic bottom is fine sandstone, with a thickness of about 5.09 m. Coal mine location is shown in Figure 1, mine underground characteristics are shown in Figure 2.



Figure 2. Mine underground characteristics

Observe the damage of surrounding rocks by using the drilling television (shown in Figure 3) of Wuhan Gude Technology Co., Ltd., which can show the characteristics of the broken coal rock mass in the form of an unrolled picture, which can be clearly seen through the drilling image (Sena et al., 2021; Zhang et al., 2019). The characteristics of fissure development have visualization effects, which make up for the lack of coal mine geology (Wang et al., 2021a; Shi et al., 2019).

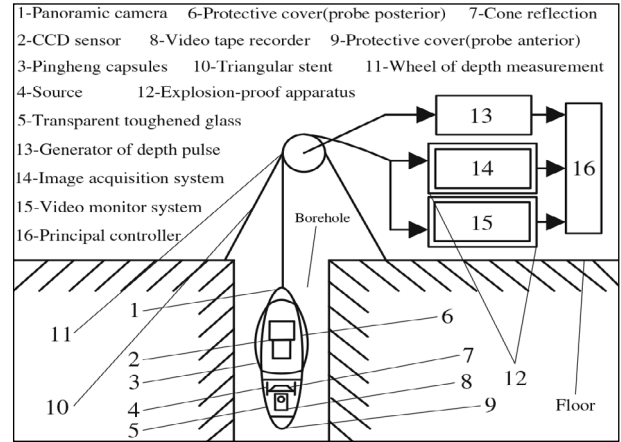


Figure 3. Structure diagram of boreholes television

The drilling TV system is mainly composed of five parts: an explosion-proof detection panoramic camera, a depth counter, an explosion-proof cable, a display and recording system, and a software system. Its working principle is that the reflector in the explosion-proof detection panoramic camera converts the drilling situation into a panoramic image (Zhang et al., 2019; Zhang and Wang, 2020; Shi et al., 2019). At the same time, the orientation information and the panoramic image are transmitted through a cable for a computer recording system (Fan, 2020; Fu and Wang, 2020; Gao, 2019). The depth counter monitors the depth of the probe in real time and transmits the depth information to the recording system (He et al., 2019; Hu et al., 2020). The software system will digitally process the panoramic image and depth information. The display system displays it as an expanded picture.

The segmented water injection device uses a self-designed single-tube double plug device. The system diagram of the segmented water injection device is shown in Figure 4.

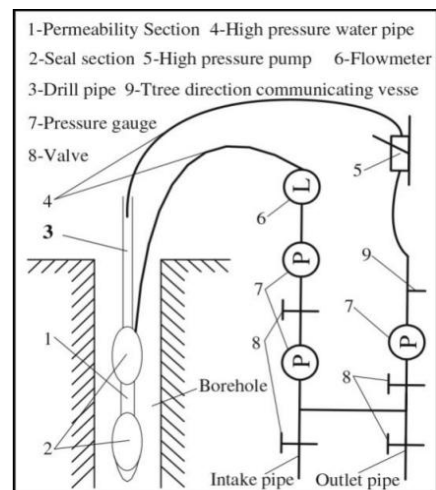


Figure 4. Zonal water injection system

The segmented water injection device is mainly composed of an operating system, a high-pressure plugging system, and a low-pressure test system (Su et al., 2020; Wang and Wang, 2021). Its working principle is that an advanced support stress will be formed in front of the working face after the coal seam is mined. When the support stress is greater than the strength of the surrounding rock, the surrounding rock will Destruction occurs and cracks are produced (Zhang et al., 2021). Because the appearance and number of cracks produced are different, the amount of water injection is also different in the same time. The characteristics of crack development are judged by comparing the water injection horizontally (Mark et al., 2021; Gamal et al., 2021).

The segmented water injection test and the drilling television use the same drilling hole. The drilling television is first performed to prevent secondary cracks in the water injection test and affect the experimental results. According to the actual characteristics of the roadway, one hole is arranged for each section, and three sections are arranged. The length of each drill hole is 11 m, and the diameter of the drill hole is 91 mm in Figure 5, the width and height of the roadway are 4500 mm and 3000 mm, respectively.

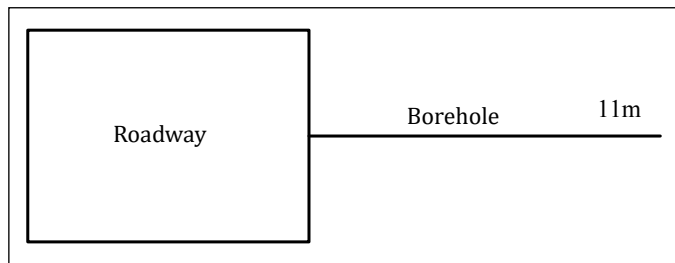


Figure 5. Schematic illustration of the layout of the peephole of the borehole television

Drilling TV detection data are shown in Figure 6.

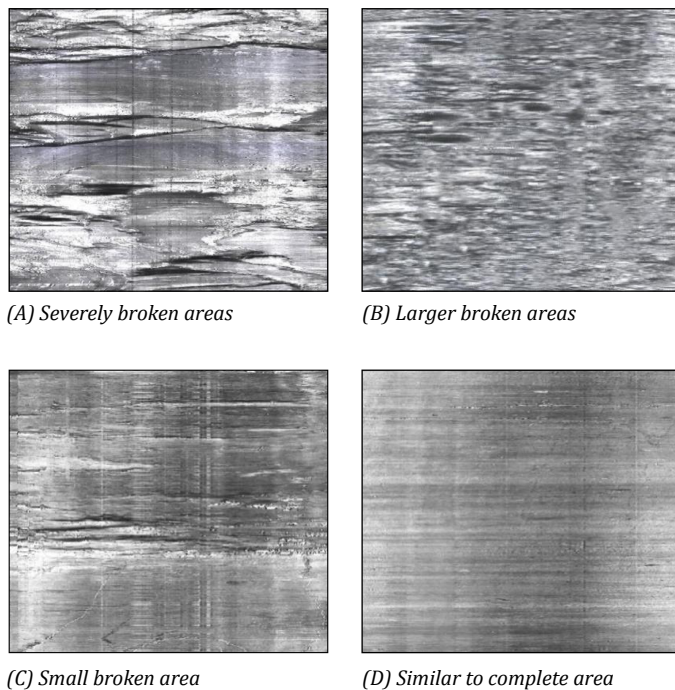


Figure 6. Characteristics of overburden fractures

2. Results

According to the fracture analysis of the drilling TV data maps in different sections, the data table shown in Table 1 is obtained.

Table 1. Fracture characteristics of different depths

Borehole depth	Fracture characteristics (I)
0.24	Big: very broken
0.42	Big: very broken
0.85	Big: very broken
1.04	Larger broken
1.26	Big: very broken
1.64-1.82	Larger broken
2.12	Larger broken
2.45-3.14	Medium fractures, crowded together
3.82	Medium broken
4.27	Medium broken
4.79-5.12	Medium fractures, crowded together
5.45	Medium broken
6.21	Small fractures
6.67	Medium fractures
7.11	Small fractures
7.47	Rimala
7.92	Micro fractures
8.25	Micro fractures
8.71	Rimala
9.25	Micro fractures
9.78	Micro fractures

The fracture development characteristics observed in the boreholes observed by the drilling television are divided according to the fracture width. As shown in Table 2, the fracture width in the severely broken area is mainly 5-9 mm, and the coal and rock body is severely broken. The phenomenon of pores; the crack width in the larger crushing zone is mainly 3-4 mm, and there are many and dense cracks; the crack width in the small crushing zone is mainly 1-2 mm, and the number of cracks is small; there are almost no cracks in the complete zone.

Table 2. Distribution characteristics of drilling fracture

Borehole number	Severely broken area /m	Larger broken area/m	Broken area/m	Similar to complete area /m
Section (I)	0-2.3	2.3-6.7	6.7-8.8	8.8-10
Section (II)	0-2.1	2.1-6.4	6.4-8.2	8.2-10
Section (III)	0-2.5	2.5-6.2	6.2-7.8	7.8-10

The water injection test data is shown in Figure 7.

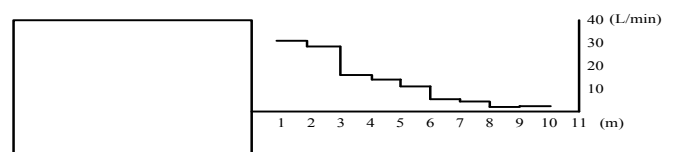


Figure 7. Segmented water injection data curve (Section I)

During the mining process, due to the influence of the advance bearing stress, the coal and rock mass in front of the working face was damaged. The water injection volume of the drilling hole decreased with the increase of the drilling depth, and it was distributed in a "step" shape, indicating that the degree of development of drilling fractures is also in this way, three turning points appeared at 3 m, 6 m, and 8 m of the horizontal borehole. According to the characteristics of water injection volume, the water injection volume of the borehole was divided into four different zones, and the development of drilling fractures in the four zones was different.

Rock Failure Process Analysis System (RFPA) is achieved by adding material heterogeneity parameters to the calculation unit. Through the accumulation of unit failure to achieve macro failure; When the element stress reaches the failure force, failure is bound to occur (Łukasz et al., 2021). At the same time, the stiffness of the damaged element is degraded, and the discontinuous problem is treated by continuum mechanics. The element property is linear elastic brittle, and the elastic modulus and strength of the element conform to normal distribution, Weber distribution and so on RFPA numerical simulation software is a numerical method that can simulate the dynamic failure of materials (Su et al., 2020). Based on the finite element and statistical damage theory, it integrates the random distribution characteristics of material heterogeneity and discontinuity, and integrates these properties of materials into the finite element method. For the element failure that meets the failure criterion, the numerical simulation of the failure of heterogeneous materials is realized. Because RFPA has unique analysis means, it can solve the problems that can not be realized by numerical simulation software in many coal and rock mass engineering (Liu et al., 2020). The mechanical parameters are shown in Table 3.

The plane strain model is used to analyze the failure characteristics of coal and rock mass during the excavation of coal and rock mass roadway. The model size is 20002mm and is divided into 4×104 units, the roadway is a rectangular roadway, the roadway width is 450 mm, 300 mm, and the roadway buried depth is 352 m. The homogeneity of elastic modulus and compressive strength is 3, and the ratio of Poisson's ratio to the average unit weight is 100. Coulomb judgment is used as the basis for unit failure. A total of 100 steps are loaded. According to the in-situ stress test, the ratio of maximum horizontal principal stress and minimum horizontal principal stress to vertical stress is 1. Therefore, the lateral pressure coefficient is 1, the initial stress in the horizontal and vertical directions is 5MPa, and the horizontal and vertical directions are increased by 0.075 mpa each step. The simulation results are shown in Figure 8.

Table 3 Mechanical parameters

Lithologic characters	Density/ kg/m ³	Compressive strength/ MPa	Angle of internal friction/°	Poisson ratio
Mudstone	2034	49.49	23	0.25
Limestone	2818	160.1	22	0.24
No.7 coal seam	1218	12.24	19	0.28
Fine sandstone	2781	120.4	23	0.22
Siltstone	2613	90.24	22	0.26

From the numerical simulation test of the excavation evolution map of the roadway, it can be known that when the roadway starts to dig, the original stress equilibrium state is destroyed, resulting in the redistribution of the stress of the roadway coal rock mass, the support stress zone is formed around the roadway, and the

phenomenon of stress concentration inside the coal rock mass. The stress concentration phenomenon mainly occurs at the roof and floor, the two sides and the four corners of the roadway. As the roadway continues to be excavated, the load continues to increase, the load capacity of the two sides of the roadway decreases, the stress exceeds the strength of the coal and rock mass, damage occurs, and the stress concentration phenomenon also moves internally. As the excavation step continues, the stress further expands, and the damage range of the two sides of the roadway coal and rock masses is further expanded. At the same time, the phenomenon of stress concentration continues to develop in depth.

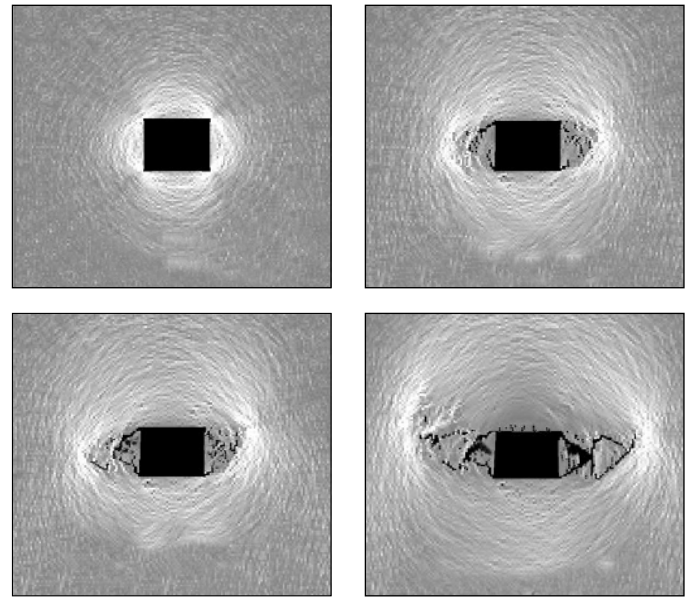


Figure 8. Evolution of tunnel excavation in numerical simulation test (Scale: 1:100)

In order to further simulate the failure characteristics of the coal and rock mass after the excavation of the roadway, and at the same time consider the influence of the actual condition of the bedding weak surface, the bedding is assumed in the simulated rock layer in advance.

From Figure 9 (A), it can be known that when the stress is 6 MPa, micro-cracks appear in the coal and rock body, and the deformation is not obvious. When the stress reaches 7.5 MPa, the two gangs undergo large damage, the roadway gangs up, and the bottom heave.

As can be seen from Figure 9 (B), the overburden of the coal seam has horizontal bedding. When the stress reaches 4 MPa, cracks occur on the roof and floor. When the stress reaches 6 MPa, stress concentration occurs, and the roof ruptures. When the stress is applied to At 7 MPa, the overburden was fractured and damaged, and at the same time, two coal and rock masses in the roadway were destroyed.

It can be seen from Figure 9 (C) that the horizontal stratification of the coal rock mass is developed. When the stress reaches 6 MPa, cracks appear on the top and bottom plates, and the stress continues to increase. When stress reaches 7.8 MPa, the two gangs protrude into the roadway, and the roof is delaminated. As the depth of the coal and rock mass increases, the crack development becomes less obvious. When the destruction depth reaches a certain depth, the rock formation has no cracks. Rock formation failure has very obvious zoning characteristics.

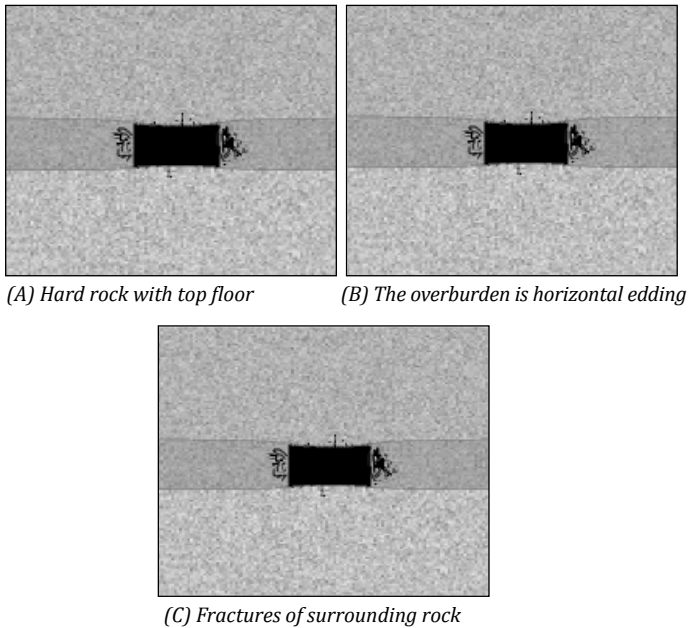


Figure 9. Numerical simulation of coal and rock breakages in roadways under different conditions (Scale: 1:100)

3. Discussion

After the excavation of the underground roadway, the original stress was broken and the stress was redistributed. The stress along the radial direction of the roadway was divided into the reduced area, the elevated area, and the original rock area (as shown in Figure 10). The influence of the advance bearing stress causes further damage to the coal rock mass in front of the working face. The joint effect of the two causes the coal rock mass to have different degrees of damage with different depths. It is mainly divided into four areas along the radial direction of the roadway: completely Crushing area, Fracture reduction zone, crushing compression area, and Proto-rock-like area.

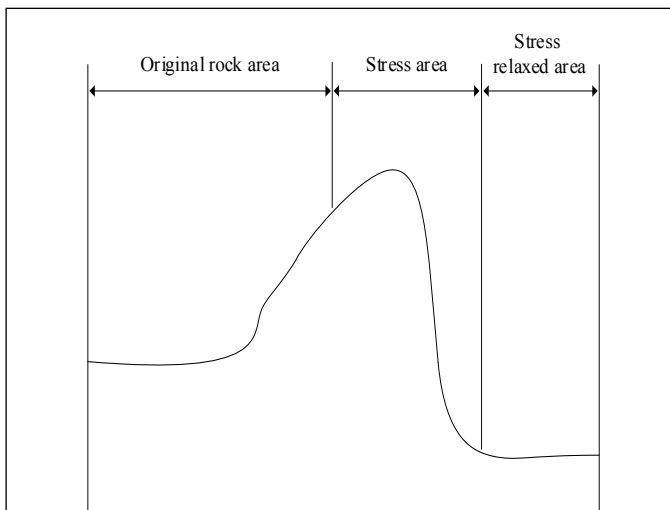


Figure 10. Characteristics of radial stress distribution in roadway

Completely broken zone: The completely broken zone is located on the surface of the coal rock body. The fractures are mainly in the vertical direction of the roadway. The primary and secondary fractures work together to make the area have a higher degree of fracture development. At the same time, the permeability anisot-

ropy is greatly reduced, with a high level of permeability. **Fracture reduction zone:** As the depth increases, the stress intensity is limited by the pressure of the coal rock mass, which is manifested as a shear effect, forming macro-shear fractures of different sizes, small and medium-sized fractures with poor connectivity, and The effect of scratches on fractured surface wounds will further reduce the permeability, which is the transition zone from high permeability to low permeability. **Fractured compression zone:** As the depth of the coal rock mass increases, the stress concentration reaches a peak. This area is affected by the dual effects of the coal rock mass and the stress concentration. The rock turns into a compression effect on the fissure, and the fissure opening is reduced. Although microscopic fissures are developed, the permeability decreases continuously along the radial direction under the restraint of high confining pressure. **Proto-rock-like area:** This area is located in the deep part of the coal rock body, and the stress is reduced to the original rock state. The stress difference between this part of the coal rock body and the original rock is relatively small. The permeability of rock formation was low.

Conclusions

The seepage field in the surrounding rock of the roadway is not only a channel for the fissure water and gas, but also a channel for the flow of the slurry during the control of the surrounding rock. Taking a mine in the Jin coal mine area as a test mine, drilling TV and segmented water injection tests were used to detect the surrounding rock failure characteristics, and the stress characteristics during the failure process were numerically simulated to study the following conclusions:

(1) Drilling television shows that the crack width of the surrounding rock can be reduced to four areas from the inside to the outside, and the crack widths are different. The surface of the surrounding rock is mainly 5-9 mm, and the coal rock body is severely broken. Mainly 4 mm, there are many dense cracks, mainly 1-2 mm inward, the number of cracks is small, and the innermost cracks are almost non-existent.

(2) The drilling water injection experiment shows that the drilling water injection volume decreases with the increase of the drilling depth and is distributed in a "step" shape. Three turning points appear at 3 m, 6 m, and 8 m. For the four different regions, the development of drilling fractures in the four regions is different.

(3) After the excavation of the roadway, the stress concentration phenomenon inside the coal rock mass appeared at the top and bottom of the roadway, the two sides and the four corners. With the excavation, the stress increased, the bearing capacity of the two sides decreased and the stress exceeded the strength of the coal rock Failure occurred, and the phenomenon of stress concentration continued to develop in depth.

(4) According to the fracture failure characteristics and stress distribution characteristics, the surrounding rock of the roadway is divided into four areas from the outside to the inside: Completely broken zone, Fracture reduction zone, Fractured compression zone, Proto-rock-like area.

References

- Cai, M.F. 2020. Key theories and technologies for surrounding rock stability and ground control in deep mining. *Journal of Mining and Strata Control Engineering*. 2(3), 033037.
- Cai, Y.F., Li, X.J., Deng, W.N., Xiao, W., Zhang, W.K. 2020. Simulation of surface movement and deformation rules and detriment key parameters in high-strength mining. *Journal of Mining and Strata Control Engineering*. 2(4), 043511.

- Chai, J., Ou, Y. Y.B., Zhang, D.D. 2020. Crack detection method in similar material models based on DIC. *Journal of Mining and Strata Control Engineering*. 2(2), 023015.
- Chen, J., Gao, J.K., Pu, Y.Y., Jiang, D.Y., Qi, Q.X., Wen, Z. J., Sun, Q.L., Chen, L.L. 2021. Machine learning method for predicting and warning of rockbursts. *Journal of Mining and Strata Control Engineering*. 3(1), 013026.
- Chen, J.W. 2020. Analysis of roadheader's rotarytable on vibration modal based on finite element method and tested data. *Journal of Mining and Strata Control Engineering*. 2(2), 026032.
- Chen, S.L., Huang, B.X., Li, D., Zhao, X.L., Xu, J., Wang, C.W. 2020. Experiment study on the basic law of high pressure abrasive hydraulic cutting for coal-rock mass. *Journal of Mining and Strata Control Engineering*. 2(4), 047521.
- Cheng, J.W., Zhao, G., Sa, Z.Y., Zheng, W.C., Wang, Y.G., Liu, J. 2020. Overlying strata movement and deformation calculation prediction models for underground coal mines. *Journal of Mining and Strata Control Engineering*. 2(4), 043523.
- Fan, K. 2020. Sudden deformation characteristic and cutting-roof support technology for double-used roadways in Longtan Mine. *Journal of Mining and Strata Control Engineering*. 2(3), 033032.
- Fu, X., Wang R.F. 2020. Cooperative self-adaptive control model of fluid feeding system and hydraulic supports in working face. *Journal of Mining and Strata Control Engineering*. 2(3), 036031.
- Gao, F.Q. 2019. Use of numerical modeling for analyzing rock mechanic problems in underground coal mine practices. *Journal of Mining and Strata Control Engineering*. 1(1), 013004.
- Gamal, R. Khaled, M. Robert, K. 2021. A coal rib monitoring study in a room-and-pillar retreat mine. *International Journal of Mining Science and Technology*, 31(1): 127-135.
- He, Y., Wang, X., Sun, H., Xing, Z., Chong, S., Xu, D., Feng, F. 2019. Coal Seam Roof: Lithology and Influence on the Enrichment of Coalbed Methane. *Earth Sciences Research Journal*, 23(4), 359-364.
- Hu, Q.F., Cui, X.M., Liu, W.K., Ma, T.J., Geng, H.R. 2020. Law of overburden and surface movement and deformation due to mining super thick coal seam. *Journal of Mining and Strata Control Engineering*. 2(2), 023021.
- Huang, F.R., Yan, S.X., Wang, X.L., Jiang, P. C., Zhan, S. B. 2021. Experimental study on infrared radiation characteristics of gneiss under uniaxial compression. *Journal of Mining and Strata Control Engineering*. 3(1), 013011.
- Jia, C., Hu C.C. 2020. Instability mechanism and control technology of longwall entries driving along the gob in a thick coal seam. *Journal of Mining and Strata Control Engineering*. 2(4), 043535.
- Kang, H.P. 2021. Temporal scale analysis on coal mining and strata control technologies. *Journal of Mining and Strata Control Engineering*. 3(1), 013538.
- Li, J.H., Li, H.J., Li, Z.C., Wu, Z.Q. 2020a. Research on river dike failure of short-distance coal seams mining under Hunchun River. *Journal of Mining and Strata Control Engineering*. 2(1), 013538.
- Li, J.K., Wang, H. 2020b. Ground support of interbedded rock roof in a deep roadway with fully-anchored cables. *Journal of Mining and Strata Control Engineering*. 2(3), 033036.
- Li, J.Y., Wang, L., Jiang, K.G., Teng, C.Q. 2021. Parameter inversion method of probability integral model based on improved wolves algorithm. *Journal of Mining and Strata Control Engineering*. 3(1), 017038.
- Li, Y., Du G. 2020c. Reasonable width of narrow coal pillars in roadway driving with gas drainage hole. *Journal of Mining and Strata Control Engineering*. 2(1), 013007.
- Liu, Y.X., Gao, M.S., Zhao, H.S., He, S.L., Li, Z.G., Zhang, Z.C. 2020. Detection of overlying rock structure and identification of key stratum by drilling and logging technology. *Journal of Mining and Strata Control Engineering*. 2(2), 023038.
- Łukasz W, Joanna K, Małgorzata K. 2021. The influence of mining factors on seismic activity during longwall mining of a coal seam. *International Journal of Mining Science and Technology*, 31(3): 429-437.
- Ma, W.Z., Zhou, X.M., Tan, S. 2020. Study on failure characteristics of coal seam floor above confined water: A case study of Shanxi Yitang Coal Mine. *Journal of Mining and Strata Control Engineering*. 2(3), 033011.
- Mark A.V.D., Ted M.K., Craig C. 2021 Coal mine entry rating system: A case study. *International Journal of Mining Science and Technology*. 31(1): 145-151.
- Ren, Y.F. 2020. Analysis and evaluation method for supporting ability of supports in coalmine working face. *Journal of Mining and Strata Control Engineering*. 2(3), 036012.
- Sena C., Ihsan B.T., Mark V. Dyke. 2021. Application of the coal mine floor rating (CMFR) to assess the floor stability in a Central Appalachian Coal Mine. *International Journal of Mining Science and Technology*, 31(1): 83-89.
- Shi, X., Zhu, S., Zhang, W. 2019. Study on the mechanisms and prevention of water inrush events in a deeply buried high-pressure coal seam-a case study of the Chensilou Coal Mine in China. *Arabian Journal of Geosciences*, 12(61419).
- Su, S.L., Du, Y., Zhu, J.F., Zhang, L., Zhao, Z.L., Meng, B. 2020. Numerical study on bearing behavior of layered rock mass for deep roadway. *Journal of Mining and Strata Control Engineering*. 2(1), 013002.
- Wang G.F., Pang Y.H., Ren H.W. 2020a. Intelligent coal mining pattern and technological path. *Journal of Mining and Strata Control Engineering*. 2(1), 013501.
- Wang J.C. 2019. Sustainable coal mining based on mining ground control. *Journal of Mining and Strata Control Engineering*. 1(1), 013505.
- Wang, D.L., Hao, B.Y., Liang, X.M. 2021a. Slurry diffusion of single fracture based on fluid-solid coupling. *Journal of Mining and Strata Control Engineering*. 3(1), 013038.
- Wang, J., Wang, X.L. 2021b. Seepage characteristic and fracture development of protected seam caused by mining protecting strata. *Journal of Mining and Strata Control Engineering*. 3(3), 033511.
- Wang, J., Zhang, C., Zheng, D., Song, W.D., Ji, X.F. 2020b. Stability analysis of roof in goaf considering time effect. *Journal of Mining and Strata Control Engineering*. 2(1), 013011.
- Wang, X.L. 2018. Research on control technology and application of grouting reinforcement of deeper fragmenting coal and rock mass. [Dissertation]. [Chengdu]: Southwest Petroleum University.
- Xu, J.L., Xuan, D.Y., Zhu, W.B., Wang, X.Z. 2019. Partial backfilling coal mining technology based on key strata control. *Journal of Mining and Strata Control Engineering*. 1(1), 013504.
- Xu, N.Z., Gao, C. 2020. Study on the special rules of surface subsidence affected by normal faults. *Journal of Mining and Strata Control Engineering*. 2(1), 011007.
- Yang, D.F., Zhang, Y.J., Wang, S., Niu, C.H., Chai, J.L. 2020. Analysis of the influence of hidden fault dip angle on ground pressure behavior in shallow seam roof. *Journal of Mining and Strata Control Engineering*. 2(4), 043038.
- Yu, X.Y., Wang, Z.S., Yang, Y., Mao, X.W. 2021. Numerical study on the movement rule of overburden in fully mechanized caving mining with thick depth and high mining height. *Journal of Mining and Strata Control Engineering*. 3(1), 013533.
- Zhang, B.L., Shen, B.T., Zhang, J.H., Zhang, X.G., 2020a. Experimental study of edge-opened cracks propagation in rock-like materials. *Journal of Mining and Strata Control Engineering*. 2(3), 033035.
- Zhang, G.J., Yan, W., Jiang, K.G. 2021. Inversion method for the prediction parameters of mining subsidence based on the PB combination prediction model of variable weight. *Journal of Mining and Strata Control Engineering*. 3(1), 013524.

- Zhang, N., Han C.L., Xie Z.Z. 2019. Theory of continuous beam control and high efficiency supporting technology in coal roadway. *Journal of Mining and Strata Control Engineering*. 1(1), 013005.
- Zhang, T., Wang, Y.L. 2020. Study on deformation evolution law and support technology of surrounding rock in multiple mining roadway. *Journal of Mining and Strata Control Engineering*. 2(2), 023016.
- Zhao, Q.C., Fu, B.J. 2020. Study on loose zone testing and support technology of roadway surrounding rock affected by dynamic pressure. *Journal of Mining and Strata Control Engineering*. 2(2), 023031.
- Zhu, W., Teng, Y.H. 2021. Study on the safety and mining influence of fully-mechanized caving mining with ultra-thick seam under Barrier Lake. *Journal of Mining and Strata Control Engineering*. 3(1), 013525.
- Zhu, W.C., Niu, L.L., Li, S.H., Li, S. 2019. Creep-impact test of rock: Status-of-the-art and prospect. *Journal of Mining and Strata Control Engineering*. 1(1), 013003.
- Zuo, J.P., Yu, M.L., Hu, S.Y., Song, H.Q., Wei, X., Shi, Y., Zuo, S.H. 2019. Experimental investigation on fracture mode of different thick rock strata. *Journal of Mining and Strata Control Engineering*. 1(1), 013007.